MAP Metric for Blind Phase Sequence Detection in Selected Mapping

Robert J. Baxley, *Student Member, IEEE,* and G. Tong Zhou, *Senior Member, IEEE*

***Abstract*—Selected mapping (SLM) is a promising technique to reduce the high peak-to-average power ratio (PAR) of orthogonal frequency division multiplexing (OFDM) signals. In this paper, we derive the optimal phase sequence detection metric for blind selected mapping (BSLM) and show that the minimum distance metric is suboptimal. We then define a certain selection criterion in the transmitter which assigns different probabilities to different mapping sequences. These probabilities are integrated into the optimal metric to achieve several dBs of SNR improvement in blind phase sequence detection.**

***Index Terms*—Orthogonal frequency division multiplexing (OFDM), peak-to-average power ratio (PAR), selected mapping (SLM).**

I. Introduction

ORTHOGONAL Frequency Division Multiplexing (OFDM) is a popular transmission method in digital communications today. It is the method of choice in many standards including 802.11a, 802.11g, 802.16, HIPERLAN 2, Digital Audio Broadcast (DAB), and Digital Video Broadcast (DVB). By partitioning a wideband fading channel into flat narrowband channels, OFDM is able to mitigate the detrimental effects of multipath interference, while maintaining a high spectral efficiency. However, the prices paid for these advantages are low power efficiencies and occasional clipping errors, which are due to the high peak-to-average power ratio (PAR) exhibited by OFDM signals.

A discrete time OFDM symbol is given by the inverse discrete Fourier transform (IDFT) of the frequency domain signal, or

$$x[n] = \frac{1}{\sqrt{N}} \sum_{k=0}^{N-1} X[k] e^{j\frac{2\pi kn}{N}}, \quad 0 \le n \le N-1 \qquad (1)$$

where $\{X[k]\}_{k=0}^{N-1} \triangleq \boldsymbol{X}$ is the frequency domain sequence drawn from a known constellation, $\{x[n]\}_{n=0}^{N-1} \triangleq \boldsymbol{x}$ is the discrete-time-domain sequence, and N is the number of subcarriers. For large N, the time-domain samples follow an (approximate) complex Gaussian distribution according to the Central Limit Theorem. The PAR of a discrete-time OFDM symbol is defined as

$$\mathrm{PAR}\{x[n]\} = \frac{\max_{0\le n\le N-1} |x[n]|^2}{E\left[|x[n]|^2\right]}. \qquad (2)$$

Notice that the expected signal power in the denominator is a constant.

Manuscript received January 5, 2005; revised June 10, 2005. This work was supported in part by the U.S. Army Research Laboratory Communications and Networks Collaborative Technology Alliance Program.

The authors are with the School of Electrical and Computer Engineering, Georgia Institute of Technology, Atlanta, GA 30332 USA (e-mail: baxley@ece.gatech.edu; gtz@ece.gatech.edu).

Digital Object Identifier 10.1109/TBC.2005.854170

Many methods have been proposed to reduce the PAR of OFDM signals. One PAR reduction approach is to modify the time-domain signal with a distortion method such as clipping [2], filtered clipping [3], and companding [4]. However, these distortion techniques are of limited use because they can induce distortion errors.

Alternatively, there are many distortionless PAR reduction methods [5]–[9]. Some use a coding scheme so that only low-PAR OFDM symbols are transmitted [5]. Other methods translate the frequency domain constellation points in order to reduce the time-domain peaks.

The distortionless PAR reduction methods work by translating the constellation points in a reversible way such that constructive interference among the constellation points is minimized. Many such methods have been proposed. Some work by applying random translation to the constellation points to see if the randomly translated points have a lower PAR than the original set of points. Selected mapping (SLM) [6], which is the subject of this paper, falls into this category. Other methods employ more complicated algorithms that try to determine which constellation points contribute to large peaks. Once the problematic constellation points are identified, they are translated to another part of the signal plane such that the peaks in the time domain are minimized [7], [8].

II. Selected Mapping

Selected mapping (SLM) [6] is a distortionless PAR reduction technique that works by alternately phasing the constellation points in order to lower the time domain peaks. By only adjusting the phase of the constellation points, the power spectrum of an SLM OFDM signal is indistinguishable from the original OFDM signal. Thus, no spectral regrowth occurs in SLM systems.

In an SLM system, a set of D phase sequences $\{\varphi^{(d)}[k]\}_{k=0}^{N-1} \triangleq \boldsymbol{\varphi}^{(d)}$ are applied to the frequency-domain symbols $\boldsymbol{X}$ to create D new sets of frequency-domain symbols $\boldsymbol{X}^{(d)} \triangleq \boldsymbol{X} \cdot e^{j\boldsymbol{\varphi}^{(d)}}$, where $\cdot$ denotes element-wise multiplication. Define $\boldsymbol{x}^{(d)} \triangleq \mathrm{IDFT}\{\boldsymbol{X}^{(d)}\}$. The PAR of each $\{\boldsymbol{x}^{(d)}\}_{d=1}^{D}$ is computed and the lowest PAR signal is transmitted. We denote the transmitted signal by $\boldsymbol{x}^{(\tilde{d})}$ where

$$\tilde{d} = \arg\min_{1\le d\le D} \mathrm{PAR}\left\{\boldsymbol{x}^{(d)}\right\}.$$

It was shown in [10] that if the D phase sequences are independent of each other and $\boldsymbol{\varphi}^{(d)}$ is drawn from a distribution such that $\mathrm{E}[e^{j\varphi^{(d)}}] = 0$, then the probability that the PAR is larger than any given threshold γ is minimized.

The set of D phase sequences is available to the receiver. However, the receiver must determine which of the D sequences was used at the transmitter. This can be done either with the transmission of side information or, as we assume in this paper,

with received-data-only processing (i.e., blindly). The latter is preferred since side information displaces bandwidth that could be used for data. Once $\tilde{d}$ is known at the receiver, the transmitted frequency domain data can be recovered by simply derotating the received frequency-domain signal with $-\boldsymbol{\varphi}^{(\tilde{d})}$.

Blind phase sequence detection was first mentioned in [6] and studied in [11]. Additionally, a novel method was proposed in [12] that integrates channel sounding and blind phase sequence detection in OFDM. The method of [12] is very effective at blindly detecting BSLM phase sequences. However, when the channel is stationary (such as in DSL, immobile wireless links, etc.) and channel sounding is not necessary for every symbol period, it is desirable to leave out the pilot tones in order to increase data rate. This stationary channel case is what the analysis in this paper applies to.

For phase sequence detection in BSLM it is assumed that both the transmitter and receiver have the set of possible phase sequences. The basic idea is that the receiver takes DFT of the received baseband signal and then uses its set of phase sequences along with some sort of metric to determine which sequence the transmitter used. Traditionally [11], it is assumed that the receiver "derotates" the received symbols and compares each derotation to the symbol constellation $\mathcal{C}$. However, it is convenient in the derivation of the detection metric to use a different, but equivalent, method.

Instead of derotating the received frequency-domain signal, assume that the received signal is compared to a rotated constellation. We will denote a rotated constellation sequence by $\boldsymbol{\mathcal{C}}^{(d)} = \{\mathcal{C}^{(d)}[k]\}_{k=0}^{N-1} \triangleq \mathcal{C} \cdot e^{j\boldsymbol{\varphi}^{(d)}}$. Notice that the constellation varies with k because the phase sequence varies with k. In other words, the receiver has to determine which of the D constellation *sequences* was used for transmission. Once the constellation is known for each subcarrier (i.e. the constellation sequence is known), then classic decoding methods can be used to determine what data was sent.

III. Ordered Phase-Sequence Testing

The power amplifier (PA) is peak power limited and is more efficient at larger input amplitudes. For simplicity, let us assume that the PA is linear up to the saturation point. Let us denote by P_{sat} the input power level beyond which saturation will occur. Denote by $P_{\max}$ the peak power of the input, and by P_{avg} the average power of the input. Clearly, clipping occurs when $P_{\max} > P_{\text{sat}}$. Cipping is a distorting operation that increases the bit error rate (BER) and/or spectral regrowth (which creates adjacent channel interference). Clipping probability is defined as

$$p = \Pr(P_{\max} > P_{\text{sat}}). \tag{3}$$

We also realize that $\text{PAR} = P_{\max}/P_{\text{avg}}$.

Since the PA power efficiency is determined by $\gamma_o = P_{\text{sat}}/P_{\text{avg}}$ (the smaller the γ_o, the higher the power efficiency), it is convenient to re-write (3) in terms of the PAR and γ_o as

$$\begin{aligned} p &= \Pr\left(\frac{P_{\max}}{P_{\text{avg}}} > \frac{P_{\text{sat}}}{P_{\text{avg}}}\right) \\ &= \Pr(\text{PAR} > \gamma_o). \end{aligned} \tag{4}$$

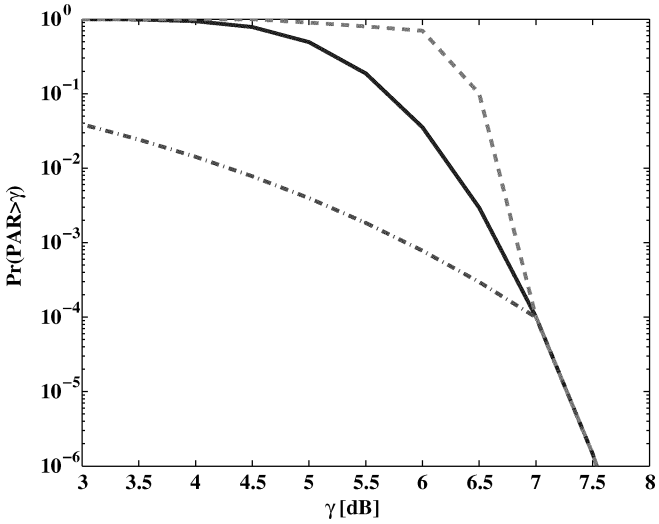

Fig. 1. Different CCDFs that all pass through the point (7 dB, 10^{-4}). In a practical system designed for a probability of clipping of 10^{-4} and clipping level of 7 dB, these curves all correspond to the same power efficiency performance.

The goal of PAR reduction is to increase power efficiency while keeping the probability of clipping at an acceptably low level. We can quantify clipping in a transmission system by p and γ_o as defined in (4). For instance, a system with $\gamma_o = 7\,\text{dB}$ that is able to tolerate at most 1 clipped OFDM block in 10,000 would have $\Pr(\text{PAR} > \gamma_o) \triangleq p = 10^{-4}$.

We assume that the PA is not adaptively biased, which means that the system is designed according to a certain P_{sat} and P_{avg}. If the PAR of a signal is small so that for example, $P_{\max} < P_{\text{sat}}$, it only means that there will be no clipping, but the power efficiency remains the same, since P_{sat} and P_{avg} are fixed in a nonadaptively biased transmission system. Once the system is designed for a certain (γ_o, p) pair, achieving a PAR value less than γ_o does not help to improve the system power efficiency.

Fig. 1 is an illustration of this concept through the complementary cumulative distribution function (CCDF) curves. Notice that all of the curves pass through the point (7 dB, 10^{-4}), but they correspond to different distributions of the PAR. For a system designed around these parameters ($\gamma_o = 7\,\text{dB}$, $p = 10^{-4}$), each of the curves has the same power efficiency and clipping probability.

The consequence of all of this analysis is that an SLM system only has to test phase sequences until a signal with a $\text{PAR} < \gamma_o$ is found. It is possible that further phase mappings could produce an even lower PAR signal, but we have just established that any additional PAR reduction will not further improve the power efficiency for a given PA with a fixed bias and probability of clipping. It is also possible that after $D_{\max}$ mappings the PAR is still larger than the clipping level, in other words, the resulting $P'_{\max} > P_{\text{sat}}$. In this case the signal is simply sent despite the fact that it will be clipped by the PA. Note, however, that $D_{\max}$ is chosen to ensure that the probability of clipping is kept to the specified (low) level.

In this paper, we will be comparing traditional SLM to ordered phase-sequence testing SLM. In each of these schemes the signals that get clipped have the same envelope distribution. Thus, they have the same clipping noise distribution, which

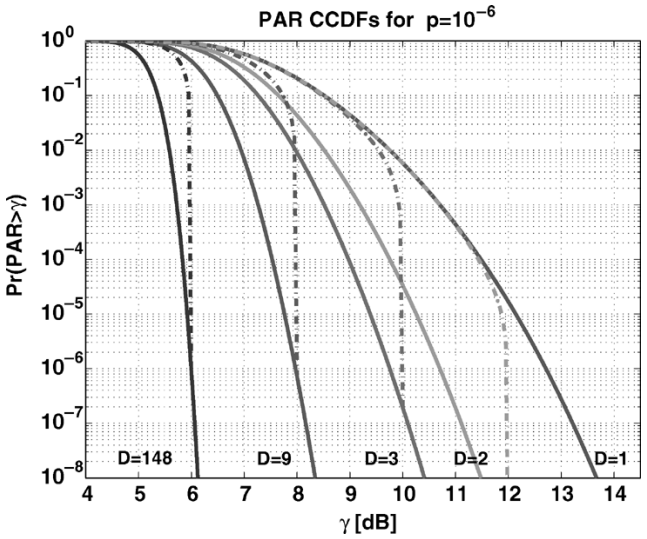

Fig. 2. Different CCDFs for $\gamma_o = \{6, 8, 10, 12\}$ dB and $p = 10^{-6}$. For each (γ_o, p) combination, the CCDFs for traditional SLM (solid lines) as well as orderer testing SLM (dashed lines) are shown. $N = 128$.

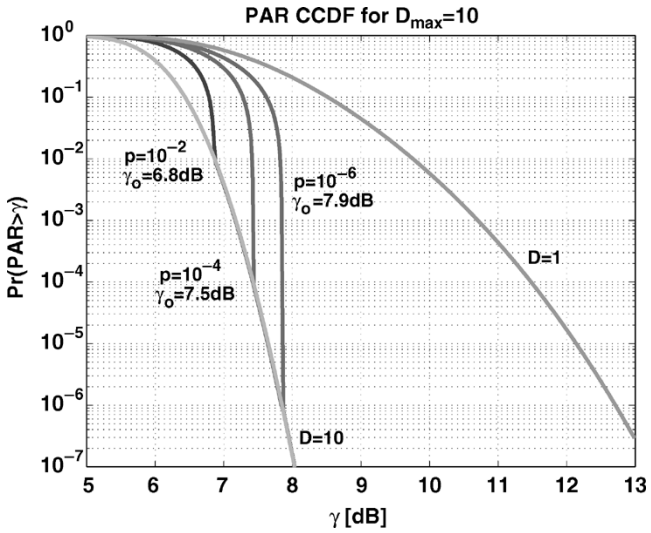

Fig. 3. Different CCDFs for $D_{\max} = 10$ and $p = \{10^{-2}, 10^{-4}, 10^{-6}\}$. $N = 128$.

means the BER increase from clipping will be identical for SLM and ordered phase-sequence testing SLM.

It has been shown in [6] that the CCDF of the PAR of a Nyquist sampled OFDM signal is

$$\Pr(PAR_{SLM} > \gamma) = \left(1 - (1 - e^{-\gamma})^N\right)^D \tag{5}$$

where N is the number of subcarriers and D is the number of independent phase mappings. For brevity we will define

$$\Gamma \triangleq 1 - e^{-\gamma}, \qquad \Gamma_o \triangleq 1 - e^{-\gamma_o}. \tag{6}$$

If the SLM process stops when $\mathrm{PAR} < \gamma_o$ then we can solve for $D_{\max}$ to guarantee that $\Pr(\mathrm{PAR} > \gamma_o) \leq p$.

$$p = \left(1 - \Gamma_o^N\right)^{D_{\max}} \tag{7}$$

$$\Rightarrow D_{\max} = \left\lceil \frac{\ln(p)}{\ln\left(1 - \Gamma_o^N\right)} \right\rceil \tag{8}$$

where $\lceil a \rceil$ is the "ceil" operation that returns the smallest integer greater than or equal to a.

In some systems it may be more appropriate to design a system around the number of mappings $D_{\max}$. This is the case when the application cannot tolerate additional computational time that extra mappings would require. If we choose the probability of clipping p to be the dependent variable, we have

$$p = \left(1 - \Gamma_o^N\right)^{D_{\max}} \tag{9}$$

and if γ_o is the dependent variable, then

$$\gamma_o = -\ln\left[1 - \left(1 - e^{\frac{\ln(p)}{D_{\max}}}\right)^{\frac{1}{N}}\right]. \tag{10}$$

In other words, there are three system parameters, $(p, \gamma_o, D_{\max})$, any two of which determine the third. Figs. 2 and 3 illustrate this concept. Fig. 2 shows several CCDFs where γ_o and p are specified and determine the value of $D_{\max}$. Fig. 3 shows several CCDFs where $D_{\max}$ and p are specified and determine the value of γ_o.

For given $D_{\max}$ and γ_o values, the probability of selecting the d^{th} mapping becomes

$$\begin{aligned}\Pr(d) &= \Pr(\mathrm{PAR} > \gamma_o)^{d-1} - \Pr(\mathrm{PAR} > \gamma_o)^d \\ &= \begin{cases} \Gamma_o^N \left(1 - \Gamma_o^N\right)^{d-1} & 0 < d < D_{\max} \\ \left(1 - \Gamma_o^N\right)^{D_{\max}} & d = D_{\max} \end{cases}. \end{aligned} \tag{11}$$

Because the phase table is known and phase mappings are performed in the same order every time, the expression in (11) is the probability that the d^{th} phase sequence was used in transmission [13]. We will show in the next section how this analysis leads to an improved sequence detection performance.

IV. Maximum a Posteriori Probability of Detection

The maximum a posteriori (MAP) probability detector seeks to maximize the probability that the d^{th} constellation sequence, $\boldsymbol{\mathcal{C}}^{(d)}$, was used in transmission given the received sequence, $\mathbf{R}$, or

$$\begin{aligned}\tilde{d}^{(\mathrm{MAP})} &= \underset{1 \leq d \leq D_{\max}}{\arg\max} \Pr\left[\boldsymbol{\mathcal{C}}^{(d)} | \mathbf{R}\right] \\ &= \underset{1 \leq d \leq D_{\max}}{\arg\max} \frac{\Pr\left[\mathbf{R} | \boldsymbol{\mathcal{C}}^{(d)}\right] \Pr\left[\boldsymbol{\mathcal{C}}^{(d)}\right]}{\sum_{m=1}^{D_{\max}} \Pr\left[\mathbf{R} | \boldsymbol{\mathcal{C}}^{(m)}\right] \Pr\left[\boldsymbol{\mathcal{C}}^{(m)}\right]} \qquad (12) \\ &= \underset{1 \leq d \leq D_{\max}}{\arg\max} \Pr\left[\mathbf{R} | \boldsymbol{\mathcal{C}}^{(d)}\right] \Pr\left[\boldsymbol{\mathcal{C}}^{(d)}\right]. \qquad (13)\end{aligned}$$

Note that the denominator in (12) is irrelevant because it does not depend on d. If we had used the conventional derotation receiver, then the denominator would have a d dependence and would have to be included in the formulation of the metric.

In an AWGN channel, the joint conditional probability density function (pdf), $f_{R[0],R[1],\ldots,R[N-1]|\boldsymbol{\mathcal{C}}^{(d)}}(r_0, r_1, \ldots, r_{N-1})$, is

$$f_{\mathbf{R}|\boldsymbol{\mathcal{C}}^{(d)}}(\mathbf{r}) = \frac{1}{Q^N} \prod_{k=0}^{N-1} \sum_{q=0}^{Q-1} \frac{1}{\pi N_o} e^{-\frac{\left\| r[k] - \hat{c}_q^{(d)}[k] \right\|^2}{N_o}} \tag{14}$$

where $N_o/2$ is the noise power, $\{\hat{c}_q^{(d)}[k] \in \mathcal{C}^{(d)}[k]\}_{k=0}^{N-1}$, and $\|\cdot\|$ represents the Euclidean distance in the complex plane. We

can substitute $\Pr(d)$ for $\Pr[\boldsymbol{\mathcal{C}}^{(d)}]$ and $f_{\mathbf{R}|\boldsymbol{\mathcal{C}}^{(d)}}(\mathbf{r})$ for $\Pr[\mathbf{R}|\boldsymbol{\mathcal{C}}^{(d)}]$ in (13) to obtain

$$\tilde{d}^{(\mathrm{MAP})} = \underset{1\le d\le D_{\max}}{\arg\max}\ \Pr(d) \prod_{k=0}^{N-1}\sum_{q=0}^{Q-1} e^{-\frac{\left\|r[k]-\hat{c}_q^{(d)}[k]\right\|^2}{N_o}} \tag{15}$$

where $\Pr(d)$ is given in (11). Notice we were able to leave out the constant terms in $f_{\mathbf{R}|\boldsymbol{\mathcal{C}}^{(d)}}(\mathbf{r})$ because of the arg max operation.

In [11] it was claimed that the optimal maximum likelihood (ML) sequence detection metric (given that the sequences are equally likely and the information modulated on each subcarrier is independent) is the minimum distance (MD) metric:

$$\tilde{d}^{(\mathrm{MD})} = \sum_{k=0}^{N-1} \underset{\substack{0\le d\le D_{\max}\\ 0\le q\le Q-1}}{\arg\min} \left\|r[k]-\hat{c}_q^{(d)}[k]\right\|. \tag{16}$$

In fact, the optimal ML metric is

$$\begin{aligned}\tilde{d}^{(\mathrm{ML})} &= \underset{0\le d\le D_{\max}}{\arg\max} \prod_{k=0}^{N-1}\sum_{q=0}^{Q-1} e^{-\frac{\left\|r[k]-\hat{c}_q^{(d)}[k]\right\|^2}{N_o}} \\ &= \underset{0\le d\le D_{\max}}{\arg\max} \sum_{k=0}^{N-1} \ln\left[\sum_{q=0}^{Q-1} e^{-\frac{\left\|r[k]-\hat{c}_q^{(d)}[k]\right\|^2}{N_o}}\right]. \end{aligned}\tag{17}$$

The suboptimal metric in (16) performs almost identically to the optimal metric in (17). This is because

$$\begin{aligned}&\underset{0\le d\le D_{\max}}{\arg\max}\ \ln\left[\sum_{q=0}^{Q-1} e^{-\frac{\left\|r[k]-\hat{c}_q^{(d)}[k]\right\|^2}{N_o}}\right] \\ &\qquad\approx \underset{\substack{0\le d\le D_{\max}\\ 0\le q\le Q-1}}{\arg\min} \left\|r[k]-\hat{c}_q^{(d)}[k]\right\| \end{aligned}\tag{18}$$

the constellation point used in the transmitter, $\hat{c}_q^{(\tilde{d})}[k]$, dominates the sum over q on the left hand side of (18). This approximation is very convenient because it significantly reduces the computational complexity of the metric. Specifically, the QN exponentiations needed for the optimal MAP metric in (15) are no longer necessary. Using this approximation, the suboptimal MAP (AMAP) criterion becomes

$$\begin{aligned}\tilde{d}^{(\mathrm{AMAP})} = \underset{0\le d\le D_{\max}}{\arg\max} \Bigg[&\ln[\Pr(d)] - \frac{1}{N_o} \\ &\times \sum_{k=0}^{N-1} \min_{0\le q\le Q-1} \left\|r[k]-\hat{c}_q^{(d)}[k]\right\|^2\Bigg] \end{aligned}\tag{19}$$

where $\Pr(d)$ is given in (11). Also, we will refer to

$$G^{(d)}(\mathbf{R}) \triangleq \ln[\Pr(d)] - \frac{1}{N_o}\sum_{k=0}^{N-1} \min_{0\le q\le Q-1} \left\|r[k]-\hat{c}_q^{(d)}[k]\right\|^2 \tag{20}$$

as the suboptimal MAP metric.

The expression in (19) requires D times as many $\|\cdot\|^2$ operations as non-SLM ML decoding. Unlike standard ML decoding, a minimum operation is necessary instead of an argument minimum operation. However, these computational increases also exist for the metric given in [11]. The only difference computationally, between the suboptimal MAP metric and the metric given in [11] is the addition of the logarithm of the a posteriori probability, $\ln[\Pr(d)]$, to the metric. But these values can by computed offline and stored for different $D_{\max}$s. So the computational difference between the suboptimal MAP metric and the metric in [11] is $D_{\max}$ extra additions.

V. Error Rate Analysis

The distribution of the metric $G^{(d)}(\mathbf{R})$ in an AWGN channel is complicated by the minimum operation. Instead of a simple noncentral χ^2 (NCCS) random variable with $2N$ degrees of freedom, it is a more complicated distribution. However, for practical values of N and for large signal-to-noise ratios (SNRs) the distribution of G is closely approximated by the NCCS distribution. Note that when $d=\tilde{d}$ the distribution approaches the central χ^2 (CCS) distribution. Additionally, the two distributions of $G^{(d)}(\mathbf{R})$ and $G^{(\tilde{d})}(\mathbf{R})$ are not independent because they share the same additive noise. There exists a bivariate noncentral χ^2 pdf and it is given in [14]. With this pdf, $f_{G^{(d)},G^{(\tilde{d})}}(x,y)$, the phase sequence detection error rate (DER) for the d^{th} mapping is

$$DER_{d,\tilde{d}} = \int_0^\infty\int_x^\infty f_{G^{(d)},G^{(\tilde{d})}}(x,y)dydx. \tag{21}$$

The DER can be extended to the $D_{\max}$ case with

$$DER = \sum_{\tilde{d}=1}^{D_{\max}} \Pr(\tilde{d}) \sum_{\substack{d=1\\ d\ne\tilde{d}}}^{D_{\max}} DER_{d,\tilde{d}}. \tag{22}$$

Despite of the simplicity of (21) and (22), there is a complication, which is that the pdf given in [14] is not amenable to numeric integration.

As an alternative, we propose to approximate $f_{G^{(d)},G^{(\tilde{d})}}(x,y)$ with a bivariate Gaussian distribution. This method can be justified by the multivariate Central Limit Theorem because both $G^{(d)}$ and $G^{(\tilde{d})}$ are sums of a large number of independent random variables [15]. Define

$$\begin{aligned} G^{(d)} &\sim N(\mu_x,\sigma_x) \\ G^{(\tilde{d})} &\sim N(\mu_y,\sigma_y) \\ \frac{\mathrm{Cov}\left(G^{(d)},G^{(\tilde{d})}\right)}{\sigma_x\sigma_y} &= \rho. \end{aligned}$$

Now

$$DER_{d,\tilde{d}} = \int_{-\infty}^\infty\int_x^\infty \frac{e^{\frac{-1}{2(1-\rho^2)}\left(\frac{(x-\mu_x)^2}{\sigma_x^2}-\frac{2\rho xy}{\sigma_x\sigma_y}+\frac{(y-\mu_y)^2}{\sigma_y^2}\right)}}{2\pi\sigma_x\sigma_y\sqrt{1-\rho^2}}dydx \tag{23}$$

however, since this has to be integrated numerically, it is preferable to find an expression for (23) that involves small finite limits of integration. Using a polar coordinate system we have

$$DER_{d,\tilde{d}} = \int_{\arctan\left(\frac{\sigma_y}{\sigma_x}\right)}^{\arctan\left(\frac{\sigma_y}{\sigma_x}\right)+\pi} \frac{e^{-\frac{\Delta\mu^2(1-\rho\sin(2\theta))}{2(1-\rho^2)(\sigma_x\cos(\theta)-\sigma_y\sin(\theta))^2}}}{2\pi\left(1-\rho\sin(2\theta)\right)}d\theta \tag{24}$$

where $\Delta\mu = |\mu_x-\mu_y|$.

Next, we have to find an expression for the means, variances and covariances for each D, N, and γ_o. Our approach is to ignore the minimum operation in the metric to derive these statistical measures and then use simulation results that implement the minimum operation to refine the analytical expressions.

We need to find the statistical properties of the metric when $d=\tilde{d}$ and when $d\ne\tilde{d}$. For a Q-ary PSK constellation with

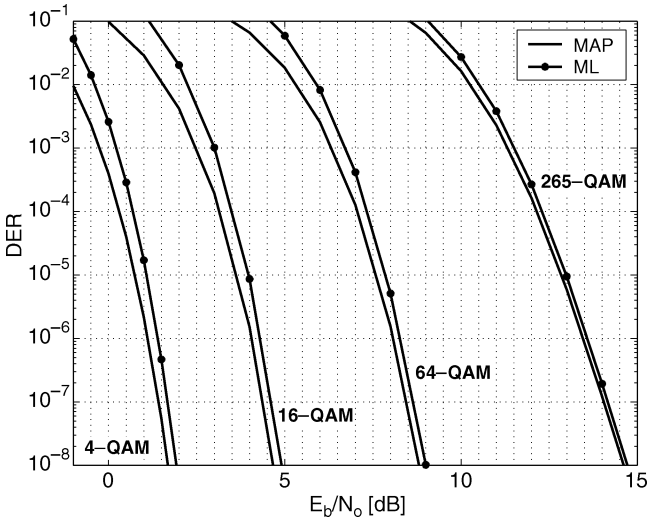

Fig. 4. Plot parameters: $N = 512, \gamma_o = 10\,\mathrm{dB}, p = 10^{-7}$, and $D_{\max} = 5$. The DER is plotted versus the bit energy to noise ratio for different constellations. For each constellation, the DER for the suboptimal ML (starred) and MAP (line) detection methods are plotted.

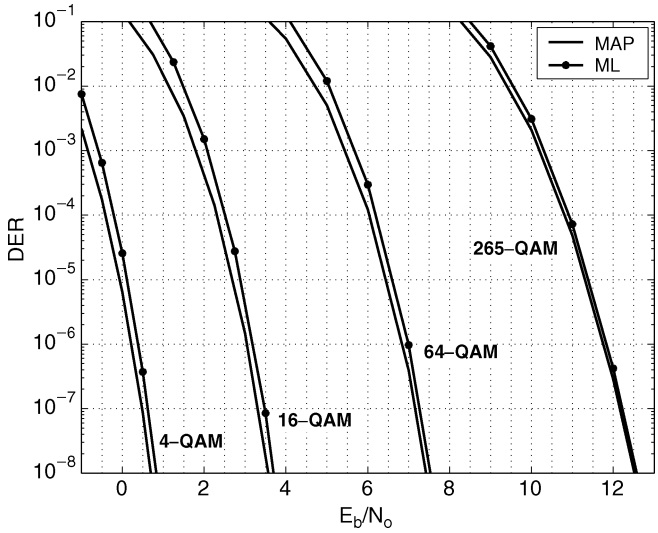

Fig. 5. Plot parameters: $N = 1024, \gamma_o = 9\,\mathrm{dB}, p = 10^{-7}$, and $D_{\max} = 14$. The DER is plotted versus the bit energy to noise ratio for different constellations. For each constellation, the DER for the suboptimal ML (starred) and MAP (line) detection methods are plotted.

constellation points at angles $\{\phi_q\}_{q=0}^{Q-1}$ and magnitude $\sqrt{E_s}$ we have

$$\mathrm{E}\left[G^{(d\neq\tilde{d})}\right] = -N - 2N\frac{E_s}{N_o}\left(1 - \frac{Q}{\pi}\sin\left(\frac{\pi}{Q}\right)\right) + \ln\left[\Pr(D=d)\right] \tag{25}$$

$$\mathrm{Var}\left[G^{(d\neq\tilde{d})}\right] = N + 2N\frac{E_s^2}{N_o^2} \times \left(1 + \frac{Q}{\pi}\sin\left(\frac{\pi}{Q}\right)\cos\left(\frac{\pi}{Q}\right) - \frac{2Q^2}{\pi^2}\sin^2\left(\frac{\pi}{Q}\right)\right) \tag{26}$$

$$\mathrm{E}\left[G^{(\tilde{d})}\right] = -N + \ln\left[\Pr(D=\tilde{d})\right] \tag{27}$$

$$\mathrm{Var}\left[G^{(\tilde{d})}\right] = N \tag{28}$$

$$\mathrm{Cov}\left[G^{(\tilde{d})}, G^{(d)}\right] = N. \tag{29}$$

where the phase angles in the phase mappings are uniformly distributed on $[0, 2\pi)$. These equations are appealing because they can be expressed in a relatively simple closed form. On the other hand, they are of limited use in that they are only applicable to PSK constellations. DSL systems use very large QAM constellations [16] which are not amenable to the sort of closed form analysis we were able to provide for PSK constellations.

Using the Gaussian error rate approximation on statistical measures derived through simulations is far easier and less time consuming than full simulations. This is because we only have to run one simulation per constellation for a range of SNRs. Because mean, variance and covariance are linear in N, it is straightforward to extrapolate these measures for any N. Furthermore, any change in $D_{\max}$ just changes the means for the metric by a known value and adds an extra term to the summation in (22). Accordingly, we have provided the best-fit lines for the statistical measures in [17].

Fig. 4 is a plot of the DER using the Gaussian approximation and the parameters from Table 1. There is a curve for each

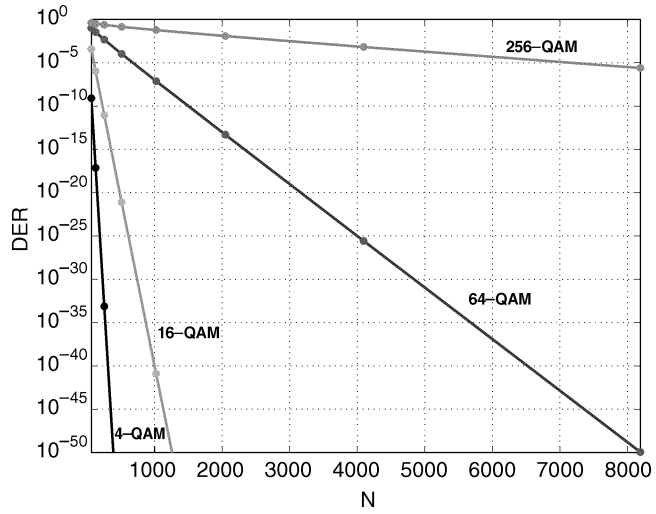

Fig. 6. Plot parameters: $E_b/N_o = 7$ dB and $D_{\max} = 5$. The DER is plotted versus the number of subcarriers, N.

constellation and for the ML and MAP metrics. The PAR reduction parameters used for the plot are $N = 512, \gamma_o = 10\,\mathrm{dB}$, $p = 10^{-7}$ and $D_{\max} = 5$ which corresponds to a 3.5 dB PAR reduction. The plot shows that by using the MAP metric, we can achieve an order of magnitude improvement in the DER. Note that this improvement is gained with negligible complexity increase ($D_{\max}$ extra additions). Fig. 5 is a DER plot with parameters $N = 1024$, $\gamma_o = 9\,\mathrm{dB}$, $p = 10^{-7}$ and $D_{\max} = 14$, corresponding to a 4.5 dB PAR reduction. The plot shows that the DER is lower even though more mappings were used, which is due to the increase in the number of subcarriers. The effect of N on the DER is illustrated more clearly in Fig. 6 where the DER with $E_b/N_o = 7\,\mathrm{dB}$ is plotted against N. We can see that the DER decreases exponentially with N when the number of mappings is held constant.

Fig. 7 is a plot of the bit error rate (BER) in an AWGN channel with a hard limiter 10 dB above the average signal power. The

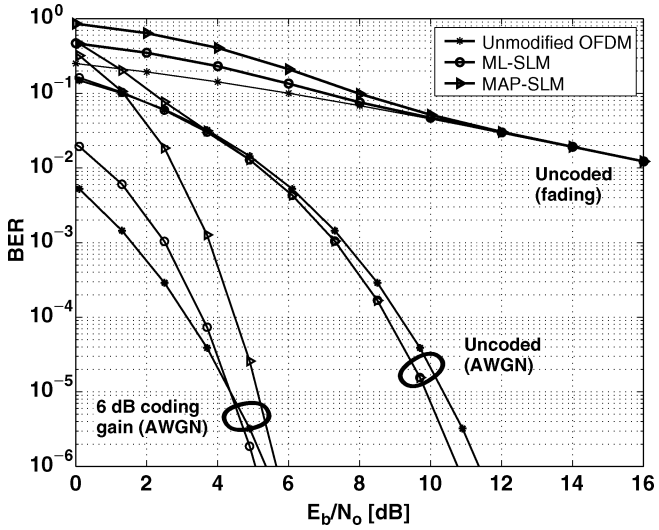

Fig. 7. Bit error rate plot for BSLM with a hard limiter and 4-QAM modulation. The BER is plotted for the uncoded and coded AWGN channel as well as the uncoded fading channel. For each case, BER is shown for the unmodified OFDM, detection with the ML criterion, and detection with the MAP criterion. Plot parameters: $N = 64$, $\gamma_o = 10$ dB, $p = 10^{-7}$, and $D_{\max} = 3$.

plot illustrates how different coding gains can affect the BER in a BSLM system. For the uncoded case the BER is dominated by errors in constellation point detection which means that the ML and MAP curves basically coincide. The OFDM without SLM curve is higher because of clipping errors incurred by the hard limiter. When a coding gain of 6 dB is used we can see a distinct difference between the three curves. Specifically, we can see that the MAP criterion has about a 0.8 dB advantage over the ML criterion at the 10^{-6} BER level. Also plotted in Fig. 7 is the BER over 30 000 random four-tap rayleigh fading channels. The curves were simulated assuming the receiver has perfect channel state information. The plot illustrates that blind phase sequence detection is robust even in fading channels, as evidenced by all three lines (MAP, ML and unmodified OFDM) coinciding above 12 dBs of SNR.

VI. Conclusions

In this paper we have presented the MAP criterion for detecting phase sequences in BSLM. In deriving this MAP criterion it was necessary to define several details about the how the transmitter and receiver operate. Specifically, the transmitter only uses as many mappings as necessary to get below the clipping level, and the receiver compares the received symbols to a rotated constellation. The first specification ensures that each mapping has a different probability, while the second allows for a simplified MAP metric. We also provided simulations to compare the MAP metric and the ML metric. We found that the MAP metric can lead to an order of magnitude improvement in the DER.

References

[1] W. Chen, *DSL: Simulation Techniques and Standard Development for Digital Subscriber Line Systems*: Macmillan Technical Publishers, 1998.

[2] D. Kim and G. L. Stuber, "Clipping noise mitigation for OFDM by decision-aided reconstruction," *IEEE Commun. Lett.*, vol. 3, no. 1, pp. 4–6, Jan. 1999.

[3] J. Armstrong, "Peak-to-average reduction for OFDM by repeated clipping and frequency domain filtering," *IEE Electron. Lett.*, vol. 38, pp. 246–247, May 2002.

[4] X. Wang, T. T. Tjhung, and C. S. Ng, "Reduction of peak-to-average power ratio of OFDM system using a companding technique," *IEEE Trans. Broadcast.*, vol. 45, no. 3, pp. 303–307, Sept. 1999.

[5] A. E. Jones, T. A. Wilkinson, and S. K. Barton, "Block coding scheme for reduction of peak to mean envelope power ratio of multicarrier transmission scheme," *IEE Electron. Lett.*, vol. 30, no. 25, pp. 2098–2099, Dec. 1994.

[6] R. W. Bauml, R. F. H. Fischer, and J. B. Huber, "Reducing the peak-to-average power ratio of multicarrier modulation by selected mapping," *IEE Electron. Lett.*, vol. 32, no. 22, pp. 2056–2057, Oct. 1996.

[7] J. Tellado, *Multicarrier Modulation With Low PAR: Applications to DSL and Wireless*: Kluwer Academic Publishers, 2000.

[8] B. S. Krongold and D. L. Jones, "PAR reduction in OFDM via active constellation extension," *IEEE Trans. Broadcast.*, vol. 49, no. 3, pp. 258–268, Sep. 2003.

[9] S. H. Muller and J. B. Huber, "OFDM with reduced peak-to-average power ratio by optimum combination of partial transmit sequences," *IEE Electron. Lett.*, vol. 33, no. 5, pp. 368–369, Feb. 1997.

[10] G. T. Zhou and L. Peng, "Optimality condition for selected mapping in OFDM," IEEE Trans. Signal Processing, 2005, submitted for publication.

[11] A. D. S. Jayalath and C. Tellambura, "A blind SLM receiver for PAR-reduced OFDM," in *Proc. IEEE Vehicular Technology Conf.*, Sep. 2002, pp. 219–222.

[12] N. Chen and G. T. Zhou, "Peak-to-average power ratio reduction in OFDM with blind selected pilot tone modulation," in *Proc. IEEE Int. Conf. Acoustics, Speech, and Signal Processing*, Philadelphia, PA, Mar. 2005, pp. 845–848.

[13] R. J. Baxley and G. T. Zhou, "Assessing peak-to-average power ratios for communications applications," in *Proc. IEEE MILCOM Conf.*, Monterey, CA, Oct. 31–Nov. 3 2004.

[14] M. Simon, *Probability Distributions Involving Gaussian Random Variables: A Handbook for Engineers and Scientists*. Norwell, MA: Kluwer Academic Publishers, 2002.

[15] W. Adams, *The Life and Times of the Central Limit Theorem*: Kaedmon Publishing Company, 1974.

[16] T. Starr, J. M. Cioffi, and P. J. Silverman, *Understanding Digital Subscriber Line Technology*: Pearson Education, 1998.

[17] R. J. Baxley, "Analyzing Selected Mapping for Peak-to-Average Power Reduction in OFDM," Master of Science Thesis, Georgia Institute of Technology, 2005.